

# Quantum Gravity on Computers

N.D. Hari Dass<sup>1</sup>

Institute of Mathematical Sciences,  
Madras 600 113, INDIA

---

<sup>1</sup>e-mail:dass@imsc.ernet.in

Some times Thomas Hardy has been compared to Dostoevski, but Dostoevski is an incomparably finer artist. If Dostoevski's works could be compared to some of say, Rubens' paintings, then Hardy's are neatly finished diagrams drawn on graph paper with ruler and compass! Compare for instance the tragedy to Tess with that of Sonia, or the culmination of the forces in Raskolnikoff's confession with the melodramatic ending of "Return of the Native". "Crime and Punishment" is more superb in its conception than even Hugo's "Les Misérables". Great as is the tragedy of Raskolnikoff, greater still is the tragedy of Sonia. She reminds us of Fantine when poverty and starvation forces her to a prostitute's life, of Ophelia in her tragic devotion of Hamlet, of Cosette in her simplicity, but to whom could we compare her when, for instance, she reads out the resurrection of Lazarus to her lover. Dostoevski himself characterizes her most delicately in the words of Raskolnikoff as he threw himself at her feet, 'I do not bow to you personally, but to the suffering humanity in your person'.

— S. CHANDRASEKHAR

# 1 Introduction

At the moment quantisation of gravity, called "Quantum gravity" for short, appears to be the last frontier in Physics. This problem has proved to be formidable both conceptually and technically. At the core of these difficulties has been the fact that the dynamical degrees of freedom here are space time geometries. It is believed by many that several difficulties in the structure of physics like the singularities (space-time) of classical general Relativity theory as well as the infinities of relativistic quantum field theories would be resolved with a successful quantisation of gravity. Though some may even question the need for quantising gravity, the widespread perception is that lack of progress in quantum gravity represents a major void in our understanding of nature.

Currently many apparently diverse approaches to this problem have surfaced. For example there are the spin-2 graviton theories built around an underlying flat space where effects conventionally ascribed to the curvature of space-time are sought to be explained as dynamical manifestations of the spin-2 quanta. Classically, these theories have been shown to account for all the effects predicted on the basis of general theory of relativity as long as the gravitational fields are not too strong or are such as to change the topology of space-time as in the case of black holes, for example. Quantisation is realised only perturbatively. A more satisfactory, but essentially equivalent, formulation consists in quantising the Einstein-Hilbert action around a fixed (usually flat) background. Here too quantisation can be achieved only perturbatively. An important aspect in which perturbative quantum gravity differs from other successful quantum field theories like QED, QCD is in the lack of renormalisability. Nevertheless, a regularised version of the quantum theory exists which is identical, as a formalism, to other regularised quantum gauge field theories.

Though QG based on the Einstein-Hilbert action is non-renormalisable in  $d = 4$ , the renormalisability "improves", in the sense that non-renormalisable counter terms begin to appear only at higher and higher orders of perturbation theory, by the inclusion of appropriate matter with enhanced symmetries called "supersymmetry". Of all such supergravity theories, the so called  $N = 8$  theory is remarkable in many respects. Apart from possible nonrenormalisability appearing only at seven loops, the matter content of these theories is uniquely fixed, making them attractive choices not only for QG but also for the unification of all fundamental forces. However, here too quantisation can only be realised perturbatively.

The fact that perturbative schemes for quantum gravity pre-select a background metric around which the fluctuations are quantised makes them rather unattractive even though they may have validity in some limited domain. The earliest approach, the canonical quantisation, avoided this pit fall. However, the technical difficulties of implementing this scheme are rather well known. In a nutshell, the theory is seen to be a constrained system with the added difficulty that the solution of the constraints needs the solution to the dynamics itself. Also, the constraints are highly nonlinear and nonpolynomial. A great ray of hope in this direction is the reformulation in terms of Ashtekar variables wherein not only do the constraints become polynomial, but the metric itself becomes a secondary object. The approach also promises to open new vistas as far as nonperturbative issues are concerned.

Finally, mention has to be made of approaches to quantum gravity based on string theory. As is well known, consistency with conformal invariance of the two dimensional world sheet theory automatically incorporates spin-2 gravitons with the added bonus that (perturbative) quantum gravity is finite in this approach. Still, a satisfactory non perturbative approach is lacking. One has to await further progress in string field theory.

The main theme of my talk today is some recent progress made in understanding some nonperturbative features of QG by using numerical simulations which I have termed "Quantum gravity on computers" in a lighter vein. The literature on even this recent development is enormous and I shall not attempt to give a full bibliographical account of this fascinating area. Instead, I shall give a few key references from which the interested reader can construct a "path of understanding".

Though recourse is made to numerics in this approach, it is derived from the finest analytical ingredients from simplicial topology, geometry, statistical mechanics etc. Before discussing the details of the numerical simulations of quantum gravity, it is worthwhile understanding how the

concepts work when applied to quantum field theories in flat space-time. There are essentially two approaches to such conventional quantum field theories : a) the *Hamiltonian approach* where the dynamical variables at each space point at a given instant of time are operators acting on a huge Hilbert space a basis for which is the well known Fock space. The short distance behaviour of the product of field operators is singular

$$\phi(x) \phi(x + \epsilon) \sim \frac{1}{\epsilon^\delta} O + \dots \quad \delta > 0 \quad (1)$$

which is a reflection of the ultraviolet divergences inherent in quantum field theories owing to the infinitely many degrees of freedom.

The major technical problem of the Hamiltonian formalism is the careful treatment of such singular operator products while maintaining the basic structure of the field theory like its symmetries etc.

The other approach is the so called *Path Integral approach*. To appreciate this approach consider the quantum mechanical description of a particle. Though the trajectory of a particle has no meaning in quantum theory, in the path integral approach, one considers the space of all possible paths and assigns to each path a weight factor (in fact a phase factor)  $e^{iS(X(t))}$  where  $S(X(t))$  is the classical action evaluated for the path  $X(t)$ . Then one forms the **path integral**

$$K(x_1, t_1; x_2, t_2) = \int DX e^{iS(X)} \quad (2)$$

where  $DX$  is a measure (the Wiener measure) for the sum over all paths. This approach can also be called the "sum over histories" approach. Every quantity that appears in the above equation is a so called *c*-number and the use of mathematically subtle operators is circumvented. However, the price one has to pay for this is the care required in constructing the measure  $DX$ . As shown by Feynman, this approach is mathematically equivalent to the Hamiltonian (or Schrödinger) approach at least when the configuration space is topologically trivial. The translation to the Schrödinger approach is codified by the spectral representation for the Kernel  $K(x_1, t_1; x_2, t_2)$

$$K(x_1, t_1; x_2, t_2) = \sum_n \psi_n^*(x_1, t_1) \psi_n(x_2, t_2) \quad (3)$$

A generalisation of this construction for the case of quantum field theory consists of replacing  $DX$  by  $D\phi$ , the measure for summing over all "histories of field configurations", and  $S(X)$  by  $S(\phi)$  the action-functional for the particular history of field configuration  $\phi(x, t)$ . The major technical problem one faces now is the construction of a meaningful measure  $D\phi$  which is an infinite dimensional analog of the Wiener measure. Even if one were to succeed in finding such a measure, the technical problem of giving a meaning to the functional integral

$$Z = \int D\phi e^{iS(\phi)} \quad (4)$$

still remains because of the oscillatory nature of the integrand. This can be overcome by the so called **Euclideanisation**.

$$t \rightarrow iX_4^E \quad iS(\phi) \rightarrow -iS_E(\phi) \quad (5)$$

As established by Schwinger, Wightman, Osterwalder, Schrader and others, there is an unique extrapolation from the results of euclidean field theory to those of Minkowski field theory, at least when the topology of spacetime is trivial. For most quantum field theories of interest on flat space-time it follows that

$$S_E(\phi) \geq 0 \quad (6)$$

so that the bothersome oscillatory factor has really been made into a damping factor. In fact, it appears that as long as the Hamiltonian of the theory is bounded from below, the euclidean action is positive semi-definite.

A notable exception to this is gravity! The euclideanised action here is

$$S_E = \int \sqrt{g} R_E \quad (7)$$

and clearly the scalar curvature of a euclidean manifold need not be positive semi-definite. We will have more to say on this later on.

Finally, the measure  $D\phi$  is made meaningful by discretising the euclidean space-time.

$$D\phi = \Pi_x d\phi_x \quad (8)$$

Now derivatives of fields in the continuum have to be approximated by finite differences, for example,

$$\partial_\mu \phi \rightarrow \frac{\phi(\vec{x}) - \phi(\vec{x} + a\vec{e}_\mu))}{a} \quad (9)$$

where  $a$  is the lattice spacing.

With these modifications the generating functional,  $Z$ , of the quantum field theory, becomes

$$Z = \int \Pi_i d\phi_i e^{-S(\{\phi_i\})} \quad (10)$$

and in this form is indistinguishable from the partition function of a classical statistical system in  $d+1$  spatial dimensions where  $d$  is the spatial dimensionality of the quantum field theory problem. This exact mapping of quantum field theory onto a classical statistical mechanical problem is at the heart of the numerical simulations to probe the non perturbative aspects of quantum field theory.

Clearly there are many choices of discrete lattices one could consider like hypercubic lattice, triangular lattice and even a random lattice. And for each such choice, there are again many ways of approximating a derivative by a finite difference. Intuitively it appears reasonable that in the continuum limit all these differences in choice should become irrelevant. In fact, if one were to simply take the limit of the lattice spacing,  $a$ , to zero in all the mathematical expressions of the discretised theory, one would recover the formal expressions of the continuous theory. This is called the 'naive continuum' limit. It is a naive limiting procedure because the resulting continuum expressions are not mathematically well defined. But it turns out that the lattice theory affords a much more subtle and meaningful limiting procedure. To appreciate this, note that as the lattice spacing  $a$  tends to zero, physically measurable length scales like Compton wavelengths of particles etc must remain finite. That is, the ratio of the physical length scale  $l_{ph}$  to  $a$  actually diverges. By scaling all dimensionful quantities  $Q$  with appropriate powers of  $a$  to make them dimensionless  $Q_L$  (for example  $m_L = m.a$ ,  $area_L = area.a^{-2}$  etc) the partition function  $Z$  can be rewritten entirely in terms of the dimensionless quantities except for an irrelevant factor. The quantity  $l_{ph}a^{-1}$  precisely corresponds to one of the many correlation lengths. Thus we see that the requirement for the existence of a continuum limit is that the classical statistical system onto which the quantum field theory has been mapped must be such that at least one of its correlation lengths diverges. But this is precisely the criterion for a statistical system to have a second or higher order (as distinguished from a first order) phase transition. Now the recipe for finding the true, as opposed to the naive, continuum limit is clear : treat the parameters of the quantum field theory like coupling constants, masses (suitably scaled to make them dimensionless) as parameters of a classical statistical system (temperature, concentration, magnetic field etc) and tune them till second order phase transition points (critical) are reached. At each of these critical points a continuum theory can be defined as follows : suppose that as the parameters are tuned to a particular set of critical values, the correlation function  $\xi$  diverges as

$$\xi \rightarrow \xi_c(\{\lambda\}) \quad \text{where} \quad \xi_c(\{\lambda_c\}) = \infty \quad (11)$$

and let  $O$  be an observable of mass dimensionality  $d$ , then  $O$  will survive the continuum limit if and only if

$$O \rightarrow \xi_c^{-d} \text{ as } \{\lambda\} \rightarrow \{\lambda_c\}. \quad (12)$$

This is called correlation length scaling. In particular, if there are two observables  $O_1$  and  $O_2$  of the same mass dimensionality surviving the continuum limit,

$$\frac{O_1}{O_2} \rightarrow c(\text{finite number}) \text{ as } \{\lambda\} \rightarrow \{\lambda_c\} \quad (13)$$

It is only the set of finite limits  $\{c\}$  that represents the observable content of the continuum theory.

It is quite clear now that the “statistical continuum limit” provides much richer possibilities than the process of naive continuum limit. For one thing, the classical statistical system equivalent to the quantum field theory could have many critical points and at each of those critical points one could define a continuum theory. Even at the same critical point, in principle one could have several distinct sets of correlation lengths such that all correlation lengths belonging to a given set have the same scaling behaviour. In such a case, each of the distinct sets can define a continuum limit resulting in inequivalent continuum limits at the same critical point. This would be a statistical mechanical realisation of inequivalent quantisations. That such a possibility can indeed happen is evidenced in the case of the three dimensional compact quantum electrodynamics on the lattice where three distinct continuum limits can be defined at the same critical point corresponding to fixed string tension, fixed mass gap or the free massless photon phase.

## 2 Numerical Simulation of Statistical Systems

There are many techniques for numerical simulation of statistical systems chief among them being i) microcanonical simulations and ii) canonical simulations. Simulations are sometimes also based on the grand canonical ensemble. The essence of the numerical simulations is to generate an ensemble of configurations and perform the so called ‘importance sampling’ according to which a suitable selection procedure is adopted such that configurations that dominate the partition function are randomly generated.

The Monte Carlo simulation of this system consists of choosing an initial configuration and a so called move (update)- that yields another configuration for each initial configuration. Denoting a move that takes the configuration  $c_1$  to  $c_2$  by  $W(c_1 \rightarrow c_2)$ , there are various restrictions on  $W(c_1 \rightarrow c_2)$  if the Monte Carlo simulation is to be reliable.

i) given a configuration  $c_1$ , *all* configurations of the system must be eventually reachable by a sequence of moves. This property is called “ergodicity”. If this property is not satisfied, parts of the configuration space are never sampled.

ii) since  $W(c_1 \rightarrow c_2)$  represents the probability of getting the configuration  $c_2$  starting from the configuration  $c_1$ , the following must hold :

$$\sum_{c_2} W(c_1 \rightarrow c_2) = 1 \quad (14)$$

$$\sum_{c_1} W(c_1 \rightarrow c_2) = 1 \quad (15)$$

Given the above two properties, it follows from an application of the Frobenius-Perron theorem that  $W$  viewed as a matrix, has maximum eigenvalue of unity, and the eigenfunction corresponding to this largest eigenvalue is the equilibrium distribution  $P_{eq}(C)$ . That is

$$\sum_{c_1} W(c_1 \rightarrow c_2) P_{eq}(c_1) = P_{eq}(c_2) \quad (16)$$

It then follows that any initial ensemble of configurations eventually evolves into the equilibrium ensemble distribution  $P_{eq}(c)$ . How quickly the initial ensemble evolves into the equilibrium ensemble distribution depends inversely on the gap between the largest eigenvalue of unity and the next largest eigenvalue.

In principle any  $W(c_1 \rightarrow c_2)$  that satisfies these requirements should result in a reliable Monte Carlo simulation of the system. In practice, however, an additional requirement is made on  $W(c_1 \rightarrow c_2)$  called the property of "detailed balance". This requirement is

$$P_{eq}(c)W(c \rightarrow c') = P_{eq}(c')W(c' \rightarrow c) \quad (17)$$

There are two obvious solutions to the requirement of detailed balance : i) heat bath :  $W(c \rightarrow c') = P_{eq}(c')$  irrespective of  $c$ . ii) Metropolis : if we write  $P_{eq}(c)$  as  $e^{-S(c)}$ , the metropolis algorithm for going from a configuration  $c$  to  $c'$  is as follows : Pick the configuration  $c'$  randomly at first : if  $S(c')$  is less than  $S(c)$  accept the configuration  $c'$  as the final configuration. If on the other hand, if  $S(c')$  is greater than  $S(c)$ , accept  $c'$  with the probability  $P e^{-S(c')}$ .

Thus a practical implementation of the Monte Carlo simulation starts with an initial configuration on which one applies a sequence of moves. Two extremes for the initial configuration are the so called *cold* and *hot* starts. In the cold start, the dynamical degree of freedom takes the same value at each lattice site while in the hot start the dynamical degree of freedom takes completely random values at the lattice sites. After applying the moves a number of times, one monitors the approach to thermal equilibrium by measuring some observable. The onset of thermal equilibrium is heralded by the constancy of the average (local) of the observable with fluctuations following the characteristics of thermal fluctuations. The constant average value should be independent of the initial configuration one started with.

Once thermal equilibrium has been reached, one again generates a sequence of configurations by making sweeps of moves throughout the lattice and computes the average values of various observables. The estimation of the statistical errors is subtle as there is no a priori guarantee that the sequence of configurations used for making measurements are statistically independent. The degree of statistical independence of subsequent configurations is estimated by the "autocorrelation time"  $\tau$ . Essentially,  $\tau$  is also the time scale that governs the speed with which the system reaches equilibrium (time in Monte Carlo simulations is simply the total number of sweeps carried out on the initial configuration). A practical way of estimating the autocorrelation time is by measuring the so called "integrated autocorrelation time". First, one measures the autocorrelation function for some observable  $O$

$$A(T) = \frac{\langle O(t)O(t+T) \rangle - \langle O(t) \rangle^2}{\langle O^2(t) \rangle - \langle O(t) \rangle^2} \quad (18)$$

The integrated autocorrelation time is given by

$$\tau_{int} = \frac{1}{2} + 2 \sum_{T'=1}^{\infty} A(T') \quad (19)$$

In practice, a lot of care has to be exercised in employing this method. Because of inherent noise,  $A(T)$  for large  $T$  only goes to a constant rather than vanishing exponentially. Because of this, a naive application of the method yields diverging  $\tau_{int}$ . Experience has shown that cutting off  $T' \sim 6\tau_{int}$  gives reliable estimates. It is fair to say that understanding autocorrelation times is more an art than a science! If the autocorrelation time is  $\tau$ , then in a sequence of  $N$  sweeps only  $N/\tau$  are statistically independent.

Since the continuum limit resides only at the critical point, where the correlation lengths diverge, autocorrelation times register dramatic increase. This is quantified by so called 'dynamic critical exponent'  $\tau \sim L^z$ , where  $L$  is the system size. Off criticality  $z \sim 0$  while at criticality  $z \sim 2$ . Thus as we go to larger and larger systems to avoid finite size effects, the autocorrelation times at criticality become  $L^2$  times autocorrelation times off criticality which are of order unity. Thus to improve statistical accuracy one would need unrealistically large computer resources. Special algorithms are needed that drastically reduce the dynamic critical exponent  $z$ . Examples of such algorithms are the cluster algorithm, multigrid algorithm etc. In terms of the eigenvalue spectrum associated with  $W((c \rightarrow c'))$ , what happens as we approach criticality is that the second largest eigenvalue begins to approach the largest eigenvalue (1). This means that the thermalisation times also become very large.

In addition to the autocorrelation effects, effects of finite size often have a critical bearing on the reliability of the results.

### 3 Quantum gravity

The dynamical degrees of freedom for the gravitational system are the metric components with the restriction that two metrics that are related to each other by a general coordinate transformation are to be identified as the same metric. Of course, when Fermionic matter is coupled to gravity, the appropriate degrees of freedom are the Vierbeins (in  $d = 4$ ) or tetrads, now with the restriction that two tetrads related by either general coordinate transformation or local Lorentz transformation are to be regarded as being physically equivalent. In the present discussion, we shall restrict attention to gravitational systems with utmost bosonic matter.

The relevant functional integral is

$$Z = \int Dg e^{-S(g)} \quad (20)$$

where  $S(g)$  is some general coordinate invariant action and has the form

$$S(g) = \alpha \int dv + \beta \int R_E dv + \gamma \int R_{\mu\nu} R^{\mu\nu} dv + \dots \quad (21)$$

$dv$  being the scalar volume element ( $\sqrt{g} d^n x$ ). The Einstein-Hilbert action corresponds to only having the second term. Thus quantising general relativity would correspond to dealing with

$$Z = \int Dg e^{-\beta \int dv R_E} \quad (22)$$

Unlike the flat space quantum field theories discussed earlier, the euclideanised action now is not positive definite because even for euclidean manifolds the scalar curvature can have any sign. There has been a variety of responses to this situation. Some of these are motivated by the observation that this instability can essentially be attributed to the so called conformal mode. To understand this, consider some fiducial metric  $g_+$  such that the scalar curvature is positive. Then a metric  $g$  can be found that is related to  $g_+$  by a conformal factor,  $g' = e^\phi g_+$ , such that the scalar curvature corresponding to  $g'$  is negative. In this manner the lack of positive semi-definiteness of the Einstein-Hilbert action can be seen to be solely due to the action of the conformal mode whose kinetic term has the wrong sign.

Some of the suggestions made to overcome this situation are : i) throw away the conformal mode altogether, ii) rotate the conformal mode into purely imaginary values thereby making the kinetic term of the rotated mode of the right sign. But both these change the theory so it is not clear that it is general relativity that one is quantising. Another tantalising suggestion, made by Greensite, is to "stabilise" the action. In effect, this amounts to a non perturbative modification of the theory whose perturbative content is exactly the same as that of the original theory. But here too one is changing the theory.

Whether the unboundedness of the action is really a sickness that ought to be cured by modifying the theory, or a feature essential to the physics of quantum gravity is something that we are yet to find out. Some have argued that though the action is bounded, the entropy factor could overcome this. For this to happen, the entropy of configurations with large negative scalar curvature has to become very small. I do not see how this is possible as one can always find a conformal factor for every positive scalar curvature configuration that would map it to a negative scalar curvature configuration. In  $d = 2$ , the unboundedness problem does not exist as  $\int \sqrt{g} R$  is the Euler characteristic of the manifold.

With these provisos, we define the problem of quantum gravity to be eqn(20). To carry out numerical simulations of this problem, we need a discretisation that still keeps the geometrical essence of the problem.

In analogy with QFT on flat spacetime, one could attempt a discretisation that would consider  $g_{\mu\nu}$  at discrete lattice points as the basic variables. Already in the case of non-Abelian gauge theories on flat space-time, such a naive discretisation is incompatible with any discrete version of the non-Abelian gauge transformation. It is well known that gravity theory has many essential features of a non-Abelian gauge theory and consequently one expects the same kind of difficulties in implementing any discrete version of general covariance. In the case of flat spacetime non-Abelian gauge theories, discretisation compatible with gauge invariance is achieved by constructing the action out of elements of the holonomy of the Yang-Mills connection around closed loops of the discretised manifold. Often, the holonomy group elements are composed of elementary group elements called "Link" variables. Such a formulation of discretised quantum gravity is certainly possible. But here we shall follow a path to discretisation that is very elegant and intrinsically geometric. Further, there is a whole body of very powerful analytical work related to it that would be indispensable to both the implementation and the subsequent interpretation of numerical simulations.

### 3.1 Geometric discretisation - Simplicial decomposition

The spirit behind this approach is that any manifold can be approximated with "arbitrary accuracy" by a so called simplicial manifold. A  $d$ -dimensional simplicial manifold is a collection of  $d$ -simplices glued along the  $d-1$  dimensional boundary simplices.

Some simplices are shown in the next figure :

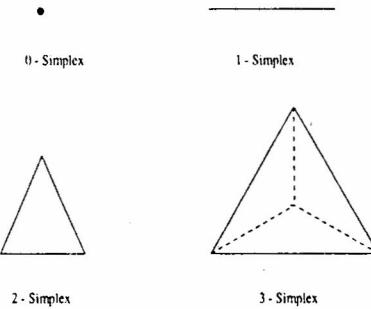


Figure 1: Some  $d$  - Simplices

A  $d$ -dimensional simplex has as its boundary  $(d+1)$  sub simplices of dimensionality  $d-1$ . As David has pointed out there are certain subtleties about gluing simplices to get a simplicial manifold. This is illustrated by the following example :

Consider the tetrahedron UNWSED and join EW. Then make the following 2-simplicial identifications : UWS  $\leftrightarrow$  UEN, UNW  $\leftrightarrow$  UES, DNW  $\leftrightarrow$  DES, DWS  $\leftrightarrow$  DEN. What one gets this way is a two dimensional simplicial complex where 2-simplices are glued to each other along 1-simplices (edges). Nevertheless, this simplicial complex is not a simplicial manifold because the neighbourhood of every vertex does not have the same topology. In fact, the boundary of the neighbourhood of  $U$  and  $D$  is  $T_2$  and not  $S_2$ . Thus one has to subject the simplicial complex to a "manifold test".

An example of a two dimensional simplicial manifold is given in the next figure. The simplicial decomposition of manifolds can be used to two rather different approaches to discretised quantum gravity. These are : i) Regge calculus, and ii) dynamical triangulation (DTR).

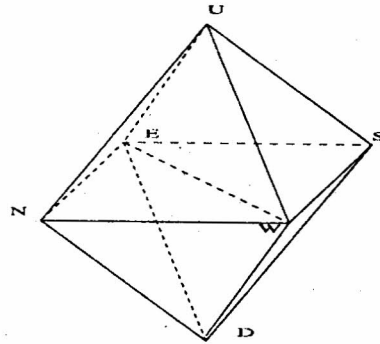


Figure 2: A simplicial complex which is *not* a simplicial manifold

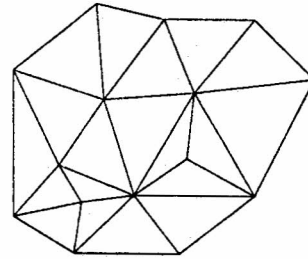


Figure 3: A simplicial complex which *is* a simplicial manifold

### 3.1.1 Regge calculus

In this approach one fixes the incidence number for each vertex (which for the two-dimensional example considered in figure 4 is simply the number of neighbours of each vertex). The length of each edge is considered as a dynamical variable and curvature is measured via deficit angles.

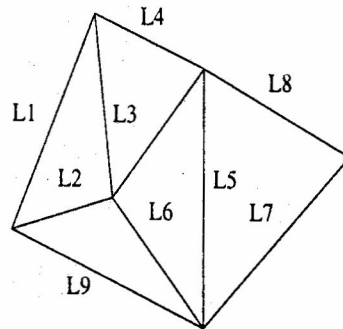


Figure 4: A Regge calculus configuration

The quantum gravity functional integral is now replaced by

$$\int Dg \rightarrow \int \left\{ \frac{dl_i}{f(l_i)} \right\} \quad (23)$$

$f(l_i)$  is the measure. As is well known, the issue of the functional measure in quantum gravity is still not very well understood. In quantum Regge calculus, this issue of the measure is further

complicated by the fact that (infinitely) many different edge length configurations correspond to the same physical manifold. This is most easily demonstrated by the example of the two dimensional flat manifold for which infinitely many Regge discretisations are possible. Starting with any given edge length configuration, one can generate all the rest by simply moving the vertices around while maintaining the various triangle-like identities. In fact, this example can be generalised to the case of any maximally symmetric space.

Numerical simulations based on Regge calculus in the case of two dimensional quantum gravity has recently been criticised for its inability to reproduce known analytical results for the so called “string susceptibility” (see discussions later in the text) for quantum gravity coupled to conformal matter. On the other hand Kawai and his coworkers have shown that some of the universal features like loop length distributions are correctly reproduced by Regge calculus method. As remarked earlier, the correct measure has not been identified and this could be at the heart of the matter. Resolution of these issues is clearly an important task for the future. For the rest of the talk I shall mainly emphasise the DTR approach.

### 3.1.2 Dynamical Triangulation (DTR)

In this approach all simplices are taken to be equilateral i.e. the edge lengths are all the same. The interior and the boundaries of all simplices and sub simplices, as in the case of Regge calculus, are considered to be flat. The manifold one gets is so called “piecewise linear”. Nontrivial curvature is produced by letting the incidence number fluctuate dynamically. The functional integral over metrics is replaced by a summation over triangulations, with some measure :

$$\int Dg \rightarrow \sum_T \frac{1}{C_T} \quad (24)$$

Again, there is no guiding principle to determine the measure,  $C_T$  ; nevertheless, results have not shown any sensitive dependence on  $C_T$ . Also, the DTR simulations in  $d = 2$  case have reproduced many of the exact analytical results.

## 3.2 Sum over topologies

In both these approaches, the issue of the topology of the manifold has to be addressed. Here again there does not appear to be any guiding principle at present. In the case of string theory represented as two dimensional quantum gravity coupled to matter, a sum over all topologies is mandatory. If on the other hand, one wishes to investigate some statistical mechanical system on a manifold with fixed topology but fluctuating metric, then one would not sum over topologies. With this in mind, the relevant functional integral will be taken to be either with a fixed topology or summed over different topologies with appropriate weight factors as the case may be.

## 3.3 Alexander Moves (updates)

With the understanding that the quantum gravity functional integral is to be replaced by a sum over all possible simplicial decompositions (also called “triangulation” from now onwards), we need to specify a move, or an update, that would take one triangulation to another. The so called “Alexander moves” provide the answer. The issue of ergodicity will be discussed shortly.

The Alexander move  $(ij, x)$  is defined as follows: take any link  $(ij)$  of the complex. Insert a new site  $x$  in the interior of  $(ij)$  and divide up the simplexes which contain  $(ij)$  into twice as many simplices, half of which replace  $i$  by  $x$  and half of which replace  $j$  by  $x$ . The inverse of this Alexander move is defined accordingly. We illustrate the Alexander move in two dimensions in the next figure.

A related concept is that of  $(k, l)_d$  moves which are defined as follows: consider a  $(d+1)$  - simplex  $S_{d+1}$  whose boundary is the collection  $\sum_d$  of  $d$ -simplices. Now partition  $\sum_d$  into collections  $\sum_1, \sum_2$  such that  $\sum_1 \cup \sum_2 = \sum_d$  and  $\sum_1 \cap \sum_2 = \emptyset$ . Since  $\sum_d$  is the boundary of  $S_{d+1}$  ( $\sum_d = \partial S_{d+1}$ ),

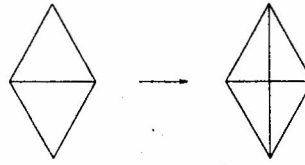


Figure 5: An Alexander move in two dimensions

the boundaries of  $\Sigma_1$  and  $\Sigma_2$  are the same but with opposite orientation. This follows from the deeper result that the “boundary of a boundary is zero” ( $\partial \Sigma_d = \partial^2 S_{d+1} = 0 \Rightarrow \partial \Sigma_1 = -\partial \Sigma_2$ ). If  $\Sigma_1$  has  $k$   $d$ -simplices and  $\Sigma_2$  has  $l$   $d$ -simplices,  $k + l = d + 2$ . The move  $(k, l)_d$  amounts to replacing  $k$  simplices of  $\Sigma_1$  by  $l$  simplices of  $\Sigma_2$ . The volume of the  $d$ -dimensional simplicial manifold is the total number of  $d$ -simplices in it; thus the  $(k, l)_d$  move leads to the volume change  $\Delta V = l - k$ . The maximum possible change of volume is  $d$ .

Let us illustrate the  $(k, l)_d$  moves by a 2-dimensional example. So we need to start with a 3-simplex which is a tetrahedron.

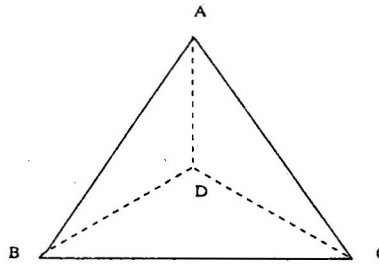


Figure 6:

The boundary of the tetrahedron ABCD is spanned by the triangles (2-simplices) ABD, BDC, DCA, ABC. thus

$$\sum_d = \{ABD, BDC, DCA, ABC\} \quad (25)$$

The inequivalent partitions of  $\Sigma_d$  we should consider are a) into 1+3, b) into 2+2. In the latter case the move leads to no change in volume.

a)  $1 \leftrightarrow 3$  :

Let  $\Sigma_1 = ABD$ ;  $\Sigma_2 = \{BDC, DCA, ABC\}$

$\partial \Sigma_1 = \text{loop}(A, B, D)$ ;  $\partial \Sigma_2 = \text{loop}(A, B, D)$  with opposite orientation.

Move  $1 \rightarrow 3$  is to start with ABD, erect the 3-simplex ABCD on ABD as base and remove ABD leading to a 2-manifold finally. This move corresponds to  $\Delta V = 2$  and an increase in the number of vertices by 1.

The inverse of this move is to locate a vertex with coordination number 3 (say D), remove the 3 triangles incident at D leaving a gap which is filled by adding the triangle ABD.

b)  $2 \rightarrow 2$  :

This can be accomplished by, say, the partition

$$\Sigma_1 = \{ABD, ABC\}; \Sigma_2 = \{BDC, ADC\} \quad (26)$$

$$\partial \Sigma_1 = \{AD, DB, BC, CA\}; \partial \Sigma_2 = -\partial \Sigma_1 \quad (27)$$

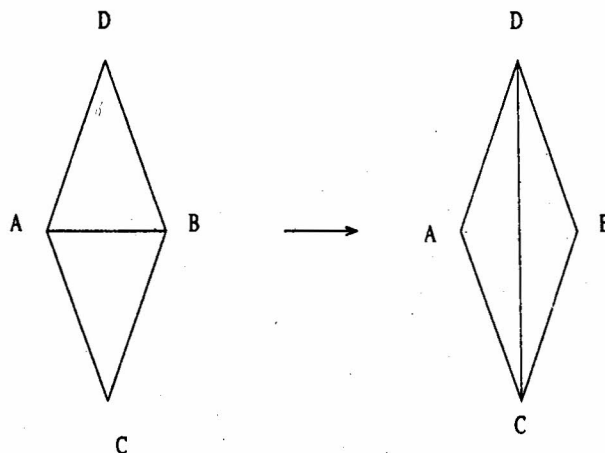


Figure 7:  $2 \rightarrow 2$  move in two dimensions

#### 4 The Dual Picture

It is often useful to introduce the dual of a simplicial manifold. Suppose we are working in  $D$  dimensions and have a simplicial manifold approximating the manifold. The simplicial manifold is obtained by gluing together  $D$ -simplices along the  $(D-1)$ -dimensional boundary simplices. Each of the  $(D-1)$ -dimensional boundary simplices has  $(D-2)$ -dimensional simplices as its boundary and so on. The 0-simplices are the vertices or sites of the discretised manifold.

The manifold dual to this is constructed as follows : to each  $p$ -simplex of the original manifold, a  $(D-p)$ -simplex of the Dual manifold is associated. If in the original manifold, two  $D$ -simplices  $V_D^1$  and  $V_D^2$  are connected along the  $(D-1)$ -simplex  $V_{D-1}^{12}$ , in the dual manifold the 0-simplices (Vertices) corresponding to them will be connected by a 1-simplex (edge) that is dual to  $V_{D-1}^{12}$ . This is illustrated below by a 2-dimensional example where the original edges are shown by bold lines and the dual edges in dotted lines :

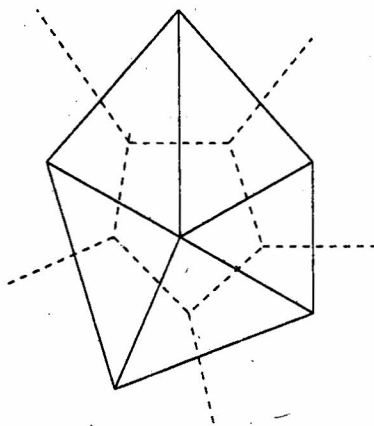


Figure 8:

It is clear that the incidence number of the dual graph is exactly  $(D+1)$ . The  $(k, l)_d$  moves get increasingly more complex as we go to higher and higher dimensions. For

example in  $d = 3$ , the possible moves are :

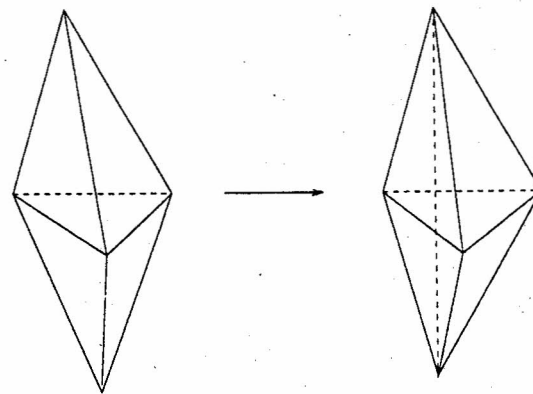


Figure 9:

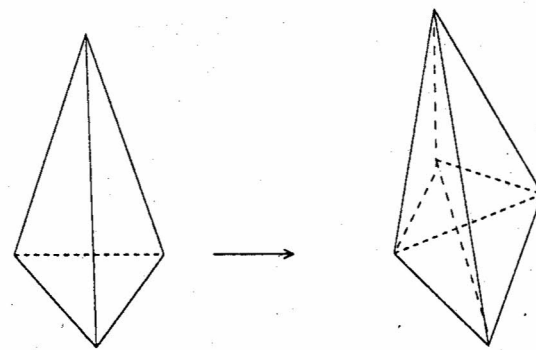


Figure 10:

These moves can be represented in a transparent manner in terms of the change in the connectivity of the dual graph. For example, the (2,2) move in 2-dimensions (the triangles are numbered)

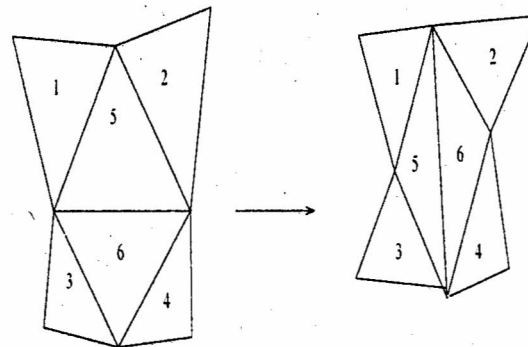


Figure 11:

has the dual representation:

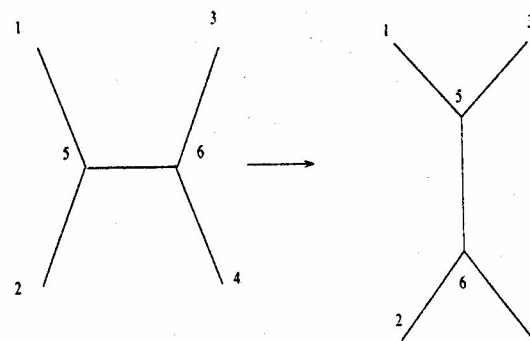


Figure 12:

Likewise, the (1,3) move

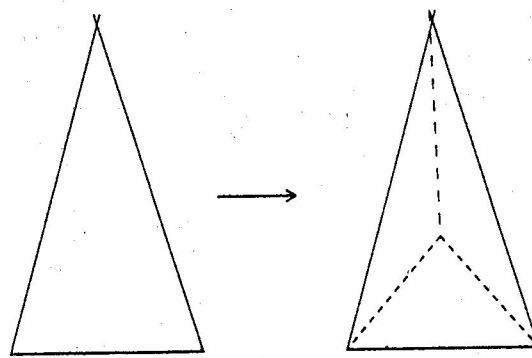


Figure 13:

has the dual representation:

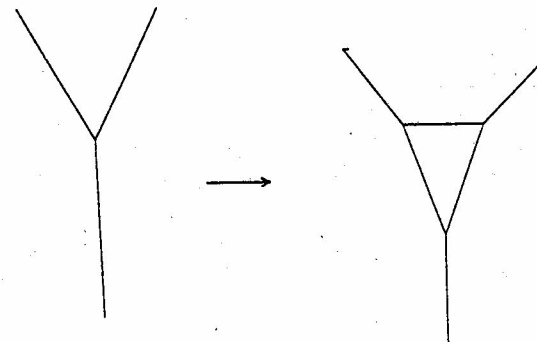


Figure 14:

The advantage of representing the  $(k, l)_d$  moves by their dual representation becomes noticeable in higher dimensions. For example, in  $d=4$ , the  $(3,3)$  move which is quite clumsy to be represented

in terms of the original simplices has the dual representation:

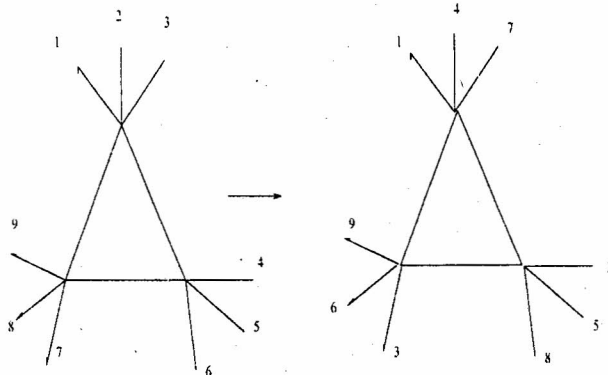


Figure 15:

## 5 Ergodicity

For the  $(k, l)_d$  moves to be useful in the Monte Carlo simulations of Quantum Gravity through the simplicial decompositions, it is necessary that they are ergodic i.e starting with some triangulation it should be possible to reach any arbitrary triangulation through a sequence of  $(k, l)_d$  moves.

For this purpose one introduces the ideas of "Alexander equivalence" and "Combinatorial equivalence" of simplicial manifolds. Two simplicial manifolds are said to be Alexander equivalent if one can go from one of them to the other through a sequence of Alexander moves. On the other hand, two simplicial decompositions are said to be combinatorially equivalent if they have a common subdivision. Now two important theorems will be stated without proof:

a) Alexander moves and  $(k, l)_d$  moves are equivalent for  $d \leq 4$ ; for  $d \geq 5$  the proof requires some additional technical assumptions (" $d - 2$ -spheres are local constructive")

b) two simplicial complexes are Alexander equivalent iff they are combinatorially equivalent.

One of the corollaries of the last statement is that any complex combinatorially equivalent to a simplicial manifold is itself a simplicial manifold.

Combining these two theorems one concludes that in  $d \leq 4$  the  $(k, l)_d$  moves are ergodic in the space of combinatorially equivalent simplicial manifolds.

### 5.1 Computational Ergodicity

There are a class of so called "computationally non-recognisable" simplicial manifolds in the sense that there is no algorithm to recognise them. For triangulations of such manifolds it can be shown that if the number of four simplices  $N_4$  of two triangulations  $T_1$  and  $T_2$  are bounded by  $N$ , the number of steps in a finite algorithm to get from  $T_1$  to  $T_2$  cannot be bounded by a recursive definable function (examples of recursive definable functions are  $N!, N!^{N!} \dots$ ). This for all practical purposes is a breakdown of ergodicity. But in simulations performed so far this has not caused any problems, but is potentially worrisome.

## 6 Action

Now that we have introduced a discretisation and a set of moves to go from one discretisation to another, we have to introduce the discrete analog of actions. Some typical actions that are general coordinate invariant are:

$$S = \int \sqrt{g} [\alpha R + \beta R^2 + \partial_\mu R \partial^\mu R + \dots] \quad (28)$$

In two dimensions  $\int \sqrt{g} R$  is a topological invariant, the Euler characteristic and its only effect is to give a weight factor depending on topology. Also,  $\int \sqrt{g}$  is the volume of the manifold, and in the context of DTR is simply the number of triangles. Therefore, for microcanonical simulations(fixed area) neither of the two terms is relevant for fixed topology simulations of random surfaces with no matter couplings. This means every configuration is equally weighted. The other terms in eqn(28) can also serve as invariant observables. To construct the discrete analogs of these terms one uses, for example,

$$R = 2\pi \frac{(6 - q_i)}{q_i} \quad \sqrt{g} = q_i/3 \quad (29)$$

In more than two dimensions all these terms are important as candidate actions: One can also think of the number of various p-simplices  $N_p$  as dynamical variables. However, not all these are independent. For example, in two dimensions  $N_1 = 3N_2/2$ . In four dimensions, one can choose  $N_2$  and  $N_4$  as independent, and a candidate action for discretised quantum gravity is

$$S = \kappa_1 N_2 + \kappa_2 N_4 \quad (30)$$

## 6.1 Two dimensional case

We shall give a very detailed account of the simulations in two dimensions as this is a very important testing ground by virtue of the availability of many different formulations as well as of exact analytical results. Before that it is instructive to consider some important aspects of the different analytical approaches available. First, let us consider the formulation according to Polyakov as well as some of the exact analytical results due to Polyakov, Knizhnik and Zamolodchikov(KPZ) on the one hand, and due to David, Distler and Kawai (DDK) on the other. The object of interest is

$$Z = \int \mathcal{D}_g X \mathcal{D}g e^{-\int \partial_\mu X \partial_\nu X \sqrt{g} g^{\mu\nu}} \quad (31)$$

In the above equation  $\mu, \nu$  take values  $1 \dots d$ , where  $d$  is the dimensionality of the Euclidean space in which the two dimensional surface is embedded.  $d$  has also the interpretation of the total central charge of the matter coupled to  $d = 2$  quantum gravity.

This model was solved exactly by Polyakov in the so called light-cone gauge, and these exact results were subsequently extended by KPZ to essentially derive all correlation functions and hence various critical exponents. It was found that the model was well defined only for  $d \leq 1$  or  $d \geq 25$ .

Of particular interest is the so called “fixed area partition function”  $Z(A)$  defined as

$$Z(A) = \int \mathcal{D}_g X \mathcal{D}g e^{-S_g(X)} \delta(\int \sqrt{g} - A) \quad (32)$$

This is essentially the number of configurations with fixed Area  $A$ . In DTR, this is studied by keeping the number of triangles fixed. The large area behaviour of  $Z(A)$  for  $c < 1$  is expected to be

$$Z(A) \sim e^{\mu A} A^{-b} \quad (33)$$

The “string susceptibility” is defined to be

$$\gamma = 3 - b. \quad (34)$$

According to KPZ and DDK, for pure surfaces ( $c = 0$ )

$$\gamma = -2 + \frac{-5\chi}{4} \quad (35)$$

More generally, for the central charge of the matter equal to  $C$ ,

$$\gamma(c) = 2 - \frac{25 - c \pm \sqrt{(25 - c)(1 - c)}}{24} \chi \quad (36)$$

where  $\chi$  is the Euler character.

The analysis of DDK also showed that in the conformal gauge, the partition function (31) is the same as that of the quantum Liouville theory :

$$Z = \int D\phi e^{-\int (\partial\phi)^2 - a \int e^{\nu\phi}} \quad (37)$$

where  $a$  and  $b$  depend on the central charge  $c$ . For  $c < 1$ , all correlation functions of the quantum Liouville theory are known.

## 7 Matrix Models

As has already been remarked upon, the graph dual to the DTR graph in  $d = 2$  has fixed incidence number of 3. Therefore, the dual graphs are Feynman graphs of  $\phi^3$  theory. The topology (Euler characteristic) of the dual graph is the same as that of the original DTR manifold. The important observation is that the generator of the  $\phi^3$  graphs with arbitrary topology can be identified with the partition function of the Hermitian  $N \times N$  - Matrix Model :

$$Z_M = \int dM e^{-tr(\frac{1}{2}M^2 + \frac{g}{6}M^3)} \equiv e^{-F} \quad (38)$$

$dM$  is the Haar measure. The asymptotic behaviour of  $F$  for large  $N$  is of the form,

$$F \sim N^2 F_0 + F_1 + N^{-2} F_2 + \dots \quad (39)$$

All  $F_i$  are singular at some  $g = g_c$  in the sense that some derivatives of  $F_i$  w.r.t.  $g$  blow up at  $g = g_c$ . A Taylor expansion of  $F(g)$  around  $g = 0$  has the form

$$F_i = \sum_{n=0} \left( \frac{g}{g_c} \right)^n a_n^{(i)} \quad (40)$$

Now the connection between this matrix model *free energy* and the fixed area partition function  $Z_\chi(A)$  for manifolds with Euler characteristic  $\chi$  is

$$Z_\chi(n) = a^{(i)} = a_n^{(i)} g_c^{-n} \quad (41)$$

with  $\chi = 2 - i$ . It is clear that  $F_i$  can also be thought of as either the free energy for a *canonical ensemble* of random surfaces with the area  $A$  playing the role of energy and  $-\log g$  playing the role of  $\frac{1}{kT}$ , or as a *grand canonical ensemble* with the number of vertices playing the role of member of particles, and  $g$  playing the role of fugacity.

The mapping of the DTR problem onto that of the matrix model can be done for central charges  $c \leq 1$ . Let us illustrate this with the example of the Ising model ( $c = 1/2$ ).

Let us consider the case where at each dual graph vertex we attach an Ising variable  $\sigma$  taking the values  $\pm 1$ . The Hamiltonian for the Ising system can be taken to be

$$H = -J \sum_{\langle ij \rangle} \sigma_i \sigma_j \quad (42)$$

where  $\langle ij \rangle$  represents the sum over all the edges of the dual-graph. It should be kept in mind that as the surfaces are updated the set of edges of the dual graph also changes dynamically. As shown by Boulatov and Kazakov, this model even in the presence of an external magnetic field is mapped onto

$$Z = \int dM_1 dM_2 e^{-tr(\frac{M_1^2}{2} + \frac{M_2^2}{2} - c M_1 M_2 + g_1 M_1^4 + g_2 M_2^4)} \quad (43)$$

The temperature and the magnetic field of the Ising system are given respectively by  $c = e^{-2J}$  and  $g_1/g_2 = e^{-2H}$ . Both the matrix models represented above are exactly solvable for  $F_i$ .

Before we give the results of DTR for various observables of interest it is instructive to recall a few features of two dimensional geometry: any metric can locally be brought to the form  $\lambda(\xi)$ -flat metric, with the help of general coordinate transformations. Naively, one would expect that if the classical action is also Weyl invariant, i.e invariant under the transformation  $g \rightarrow \lambda(x) \cdot g$ , the metric can everywhere be brought to the flat form. However, this is not true as it is impossible to find measures  $D_g X$  and  $Dg$  which are invariant under both general coordinate transformations as well as Weyl transformations. Also, on purely geometric grounds it can be shown that there are "conformal classes" of metrics so that a metric belonging to one class can not be transformed into a metric of another class by a globally well-defined Weyl transformation. When the genus  $g$  is greater than two, there are  $2g - 2$  complex parameters describing the conformal classes. For genus one (Euler characteristic zero) case, the conformal class is parametrised by a single complex parameter called moduli, and the partition function takes the form

$$Z = \int d\tau f(\tau) \quad (44)$$

The function  $f(\tau)$  is calculable.

## 8 Observables

There are several observables of interest that can be studied under DTR. Let us start with the **String Susceptibility**  $\gamma$ . It has already been defined in eqn(34). Both the continuum theory as well as the matrix model predict that  $\gamma = -1/2$  for the pure surface theory ( $c = 0$ ), and that  $\gamma = -1/3$  for the Ising model coupled to random surfaces at the critical point of the Ising system (these results are for the zero genus case). As the Ising model coupling is varied what one finds in DTR are: for  $J > J_c$  and  $J < J_c$ ,  $\gamma$  stays at  $-0.5$  and at  $J = J_c$  it reaches  $-1/3$ . Of course there is a well defined cross-over region.

It is interesting that the Ising model coupled to random surfaces is exactly solvable in the presence of an external magnetic field also, while the analogous problem in flat space remains unsolved.

In addition to the string susceptibility, one can study various critical exponents  $\alpha, \beta, \delta, \nu$  for the Ising system. One can also study the magnetic susceptibility and exponents associated with it (the precise manner the magnetic susceptibility diverges with the system size at the critical point, for example). In flat space it is well known that there are scaling relations among these various exponents that are dimension dependent. It is also known that the dependence on dimensionality appears only through the combination  $\nu d$ . The exact results based both on the continuum theory and the Matrix models predict the exponents  $\beta = 1/2, \gamma = 2$  and  $\delta = 5$  while the Onsager values are  $\beta = 1/8, \gamma = 7/4$  and  $\delta = 15$ . DTR has indeed confirmed these predictions and the validity of the scaling relations. While for the flat-space case  $\nu d = 2$  with  $\nu = 1$ , for random surface case  $\nu d = 3$ . However,  $\nu$  is not known for the random surface case. It appears as if the relevant dimensionality is the "Hausdorff dimensionality".

It is puzzling that simulations based on Regge calculus do not seem to be reproducing the exact results of the continuum and Matrix models.

### 8.1 Hausdorff Dimension

This is another quantity of interest and perhaps one of the most important lessons one has learnt from numerical simulations is that quantum fluctuations can drastically alter the scaling dimension of space-time. In flat two dimensional space through the relation  $area = \pi \cdot R^2$  for a circle, one identifies the scaling dimension to be 2. For the case of fluctuating geometry one expects  $A = \pi R^{d_H}$  where  $d_H$  is the Hausdorff dimension. The way to measure  $d_H$  in DTR is best illustrated with the

dual graph: One starts at some site of the dual graph which is marked ‘zero’ to denote the ‘origin’. Then, one marks all the neighbouring sites of the origin as ‘1’, and all the distinct neighbours of the 1-sites as ‘2’ and so on. The marking on the sites is analogous to ‘radius’ and the total number of sites with markings  $\leq R$  is taken as a measure of the area. One has to make sure that it is a connected domain. The typical results for the measurement of fractal dimensions are shown in the next figure.

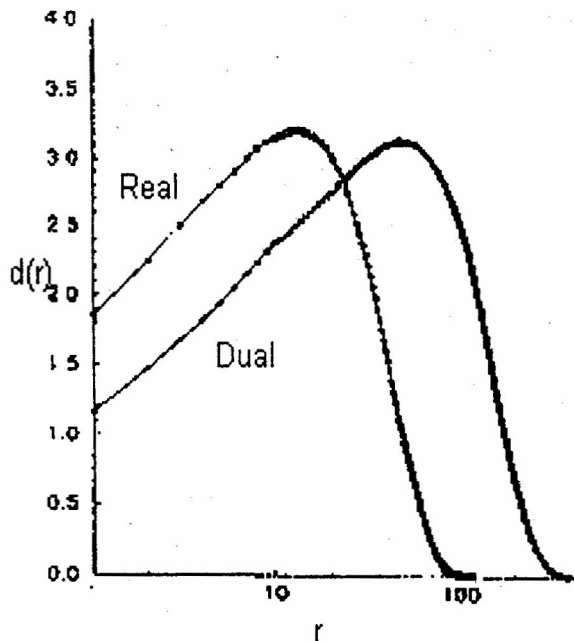


Figure 16: The numerical results of fractal dimensions measured in the real and dual spaces consisting 400,000 triangles.  $r$  represents an averaged geodesic distance.

The fractal dimension starts off at some low value, reaches a peak and starts falling off. This fall off to zero is a purely finite size effect as eventually all the triangles(dual sites) get visited. It is expected that as the system size increases, the measured fractal dimension approaches  $d_H$ . From the present simulations it appears that  $d_H = 4$  for all  $c \leq 1$ .

## 8.2 Spectral Dimension

Another intrinsically geometric quantity of interest is the so called “spectral dimension”. This is defined through the return time for a random walk. One essentially computes the kernel  $K(\vec{X}, T = 0; \vec{X}, T = T)$  and study it in the limit  $T \rightarrow 0$

$$\langle \text{Tr}K(T) \rangle \sim T^{-d_s/2} \quad \text{as } T \rightarrow 0 \quad (45)$$

Simulations indicate that  $d_s = 2$ .

## 8.3 Loop Length Distributions

Recall the introduction of the ‘radial’ distance in connection with the definition of the Hausdorff dimension. What one finds typically at a given radial distance is not just one connected domain but many, as shown in the figure below. Kawai and coworkers have shown for the pure surface

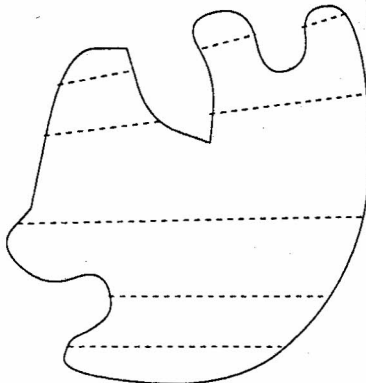


Figure 17:

case that the number of loops  $N(D)$  of perimeter  $L(D)$  at radial distance  $D$  have a universal distribution

$$N(D)D^2 = f(L(D)/D^2) \quad (46)$$

they were also able to compute the function  $f$ . Next figure shows the agreement between theory and simulations. Though the Regge calculus simulations have not been successful in reproducing the

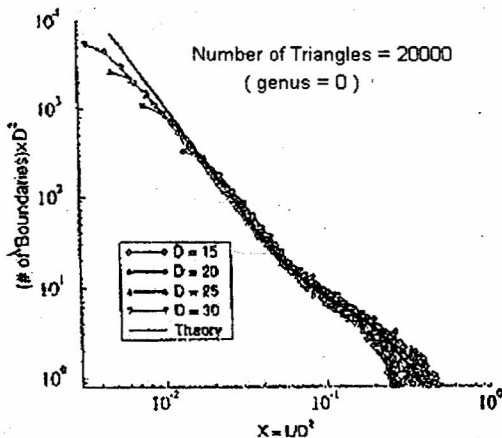


Figure 18: Loop-length distributions with Double-Log scales. The total number of triangles is 20,000 and is averaged over 500 configurations.  $X = \ell(D)/D^2$  is a scaling variable, where  $D$  represents the geodesic distance (it was measured at steps  $D = 15, 20, 25$  and  $30$ ) and  $L(D)$  represents each loop length at step  $D$ . The small circles, triangles and quadrangles indicate the results of the numerical simulations, and the solid line indicates that of string field theory.

critical exponents, they have been reasonably successful in reproducing the loop length distributions for small loops. Thus Regge calculus is perhaps not all together on the wrong track. There is also perhaps a connection between the failure of the Regge calculus in reproducing the critical exponents and its inability to capture the correct loop length distribution for large loops.

## 8.4 Baby Universes

A typical configuration produced in DTR simulations looks nothing like a smooth surface; in fact, what one finds often are various surfaces connected to each other through “necks” as illustrated in the next figure. The minimum neck size in DTR is of course a triangle and it is in fact just

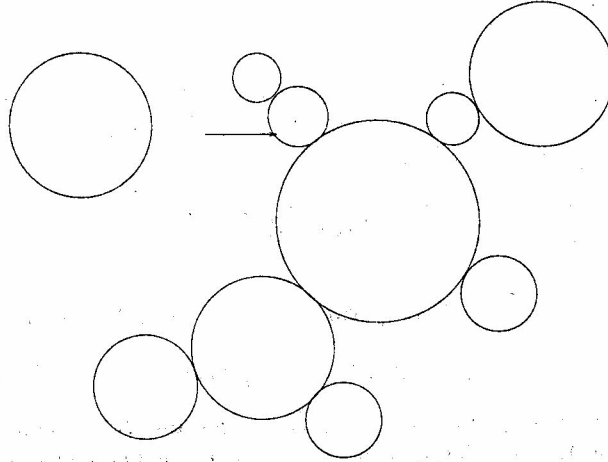


Figure 19:

a matter of counting, as shown by Jain and Mathur, to estimate the number of “minimum neck baby universes” (MINBU) once the fixed area partition sum  $Z(A)$  is known

$$n(B, A) = \frac{3(A - B + 1) Z(A - B + 1) (B + 1) Z(B + 1)}{Z(A)} \quad (47)$$

where  $n(B, A)$  is the probability of finding a MINBU of area  $B$  in a surface of total area  $A$ . This follows from the fact that a triangle can be located on a surface of area  $(B + 1)$  (1 represents the neck) in  $Z(B+1)$  ways and this can be glued at any of the  $(A + B - 1)$  locations of the surface with area  $(A - B + 1)$  along with 3 ways of gluing a triangle onto a triangle.

It is clear that counting the MINBU distribution is a very practical way of measuring the string susceptibility  $\gamma$ . However, one has to be careful about the influence of finite size corrections. From the definition of  $\gamma$  (eqns. 33, 34) it is clear that when  $\gamma \leq 0$ , the average MINBU size goes to a constant as the area of the configuration becomes larger and larger, whereas for  $\gamma \geq 0$  the average MINBU size grows with  $A$ .

As was mentioned earlier update algorithms should be able to effectively overcome critical slowing down. In simulations of spin systems on fixed geometry this is achieved through cluster algorithms and the like. In random surface simulations this problem of large autocorrelation lengths is quite serious. Ambjorn and coworkers have suggested “MINBU surgery” as a way of overcoming this. This amounts to cutting away the MINBU’s and stitching them onto the surface in arbitrary ways.

Among other observables of interest one could think of various powers of the incidence number  $q_i$ . Of course it follows rather trivially that the average coordination number is 6, in other words the average curvature (scalar) is zero.

## 8.5 Resistivity

Kawai and coworkers have proposed the use of resistivity measurements as a probe of both the smoothness of a surface as well as for determining its complex structure. For the sphere topology for which the complex structure is trivial, consider the arrangement shown in the figure. Each

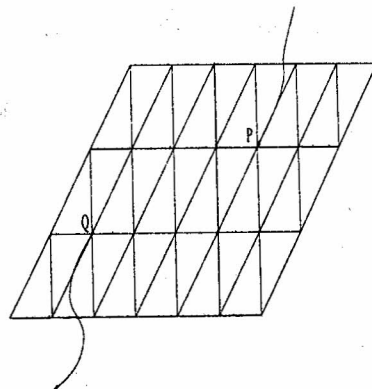


Figure 20: A resistive network

edge of the dual graph is treated as a resistor of some given resistance say 1 ohm. At the point P a current of 1 Amp flows into the surface and at the point Q a current of 1 Amp flows out. The action is modified through the addition of

$$S' = \int \sqrt{g} g^{\mu\nu} \partial_\mu V \partial_\nu V \quad (48)$$

$V$  can be thought of as an external (non dynamical) scalar field. Now one solves the discrete version of Poisson's equation for the values of  $V$  at the sites of the dual graph. One compares this with what is expected of a continuous surface

$$V(z) = \text{const} \log \frac{(z - z_P)}{(z - z_Q)} \quad (49)$$

the constant being a measure of the resistivity. This enables one to attach complex coordinates  $z$  also. Since  $\sqrt{g} g^{\mu\nu}$  is independent of the conformal factor, this method is sensitive only to the complex structure.

If the surface is a smooth surface one expects a peaking in the observed resistivity whereas for a structure like a branched polymer (to which the surface is conjectured to degenerate into when  $c > 1$ ) the distribution in resistivity is expected to be broad. In the next figure some typical DTR data for resistivity is shown: (The vertical axis is the number of configurations with average resistivity,  $r$ .)

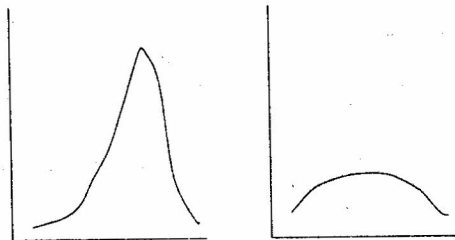


Figure 21:

## 8.6 Complex Structure

Kawai has also proposed a way of determining complex structure through resistivity measurements. First let us briefly discuss what complex structure means in the case of genus 1 topology (torii).

In the continuum picture the torus is equipped with a 'homology basis' of a-cycles and b-cycles as shown in the figure;

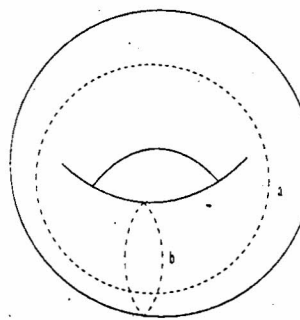


Figure 22:

Now there exists a so called Abelian differential satisfying

$$\partial_{\bar{z}}\omega = 0 \quad (50)$$

where  $\omega$  is a one form. The complex moduli  $\tau$  is defined as the ratio

$$\tau = \frac{\oint_b \omega}{\oint_a \omega} \quad (51)$$

The proposal for determining  $\tau$  through DTR is as follows: first locate the a and b cycles on the configuration. This is done by starting at  $t = 0$  with a triangle and evolving it in 'radial time' as described in the context of the Hausdorff dimension. As  $D$  increases, this elementary loop will split into other loops or stays as a single loop. If the topology is that of a sphere, all the loops will eventually shrink to their minimum size(triangle), and there will never be an instance of two loops merging into a single loop as shown in figure 23.

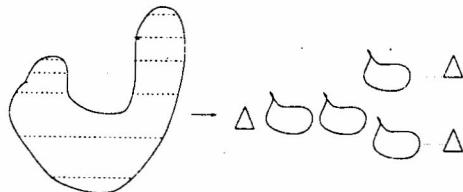


Figure 23:

On the other hand, in the case of torus topology, two loops will merge. This is shown in the figure 24:

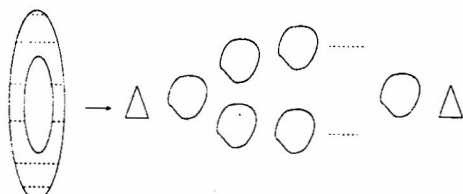


Figure 24:

The point where two loops merge will be a point on the, say, a-cycle. One of the two loops merging there can then be identified with the other(b) cycle. The entire a-cycle can now be reconstructed by following the history of the two loops that merged.

After locating the a, b-cycles, now apply a potential difference across the a-cycle and solve for the voltage distribution. On identifying

$$j_\mu = \partial_\mu V \quad (52)$$

then

$$\oint_a j = \Delta V \quad (53)$$

Now the dual of the one form  $j$  is given by

$$\tilde{j}_\mu = \epsilon_{\mu\nu} j^\nu \quad (54)$$

The holomorphic one-form  $j + \tilde{j}$  is seen to be an Abelian differential (care should be taken to include some resistivity dependent factors). Now the moduli  $\tau$  can be measured and the function  $f(\tau)$  determined. This way, Kawai, Tsuda and Yukawa have determined the bosonic string partition function for the  $c = 0$  case and it is reproducing the expected features.

## 8.7 Other Results

There are too many interesting results to report on here for lack of time, so I will just include a few examples. For example, Tsuda and Yukawa have studied the phase diagram for two dimensional gravity in the coupling constant space  $\alpha, \beta$  where

$$S(g) = \beta \int d^2x \sqrt{g} R^2 + \alpha \int d^2x \sqrt{g} g^{\mu\nu} \partial_\mu R \partial_\nu R \quad (55)$$

The phase diagram obtained is shown in the next figure:

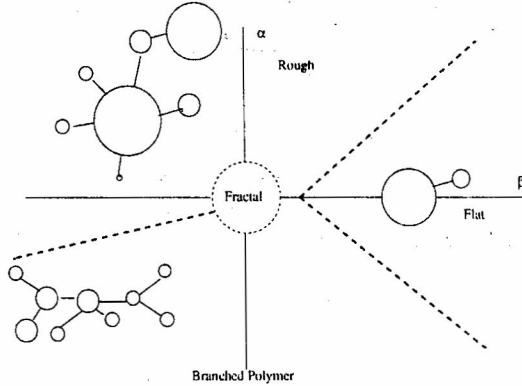


Figure 25: A phase diagram for 2d gravity

There are also some preliminary results that have been obtained by Bakker and Smit for four dimensional gravity. There is also some recent interesting work on the meaning of fixed geodesic distance in  $d = 2$  quantum gravity by H. Aoki et al.

## References

- [1] *General Relativity Without Coordinates*, T. Regge, Il Nuovo Cimento, **XIX**, No 3 (1964);
- [2] *Dynamical Triangulation - A gateway to QG ?*, J. Ambjorn, hep-th/9503108;
- [3] *Recent Progress in the theory of Random Surfaces and Simplicial QG*, J. Ambjorn, Lattice '94;
- [4] *Ising Transition in 2-d Simplicial QG, can Regge calculus be right ?*, C. Holm and W. Janke, Lattice '94;
- [5] *Regge skeletons and quantisation of 2-d gravity*, W. Bock ,Lattice '94;
- [6] *Fractal Structure in 2-d Quantum Regge Calculus*, Jun Nishimura and Masaki Oshikawa, Phys. Lett. **B 338**, 187-196, (1994);
- [7] *On the fractal structure of two-dimensional QG*, J. Ambjorn et al, hep-lat/9507014;
- [8] *Simplicial QG and Random Lattice*, F. David, Saclay Preprint T93/028;
- [9] *Simplicial Quantum Gravity*, B. V. de Bakker, Thesis submitted to University of Amsterdam, hep-lat/9508006;
- [10] *Numerical Analysis of 2-d QG*, N. Tsuda, Thesis submitted to Tokyo Institute of Technology, (1994);
- [11] S. Jain and S. Mathur, *Phys. Lett.* **B286**, 239,(1992);
- [12] For discussion of Ergodicity see:  
A. Nobutovsky and R. Ben - Av, *Comm. Math. Phys.* **157**, 93-97, (1993);  
Gross M, Varsted S, *Nucl. Phys.*, **B378**, 367, (1992);
- [13] H. Kawai, N. Kawamoto, T. Mogami and Y. Watabiki, *Phys. Lett.* **B306**, 19, (1993);
- [14] *Complex Structure of 2-d surfaces*, H. Kawai,N. Tsuda and T. Yukawa in Lattice' 95, hep-lat/9512014;
- [15] *Operator Product Expansion in 2-d QG*, H. Aoki et al, hep-th/9511117;
- [16] D. Boulatov and V.A. Kazakov, *Phys. Lett.* **B186**, 379, (1987);
- [17] N. D. Hari Dass, B.E. Hanton and T. Yukawa, *Phys. Lett.* **B368**, 55, (1996).